

# Weak Metallic Emission Lines in Early B-Type Stars

Kozo SADAKANE,<sup>1</sup> and Masayoshi NISHIMURA<sup>2</sup>

<sup>1</sup>Astronomical Institute, Osaka Kyoiku University, Asahigaoka, Kashiwara-shi, Osaka 582-8582

<sup>2</sup>2-6, Nishiyama-Maruo, Yawata-shi, Kyoto 614-8353

\*E-mail: sadakane@cc.osaka-kyoiku.ac.jp

Received ; Accepted

## Abstract

Previously unrecognized weak emission lines originating from high excitation states of Si II (12.84 eV) and Al II (13.08 eV) are detected in the red region spectra of slowly rotating early B-type stars. We surveyed high resolution spectra of 35 B-type stars covering spectral sub-types between B1 and B7 near the main sequence and found the emission line of Si II at 6239.6 Å in all 13 stars having spectral sub-types B2 and B2.5. There are 17 stars belonging to sub-type B3 and seven stars among them are found to show the emission line of Si II. The emission line of Al II at 6243.4 Å is detected in a narrower temperature range ( $T_{\text{eff}}$  between 19000K and 23000 K) in nine stars. Both of these emission lines are not detected in cooler ( $T_{\text{eff}} < 16000$  K) stars in our sample. The emission line of Si II at 6239.6 Å shows a single-peaked and symmetric profile and the line center has no shift in wavelength with respect to those of low excitation absorption lines of Si II. Measured half width of the emission line is the same as those of rotationally broadened low excitation absorption lines of Si II. These observations imply that the emitting gas is not circumstellar origin, but is located at the outermost layer of the atmosphere, covering the whole stellar surface and co-rotates with the star.

**Key words:** Stars: B-type— Stars: atmosphere — Stars: emission line— Stars: spectroscopy

## 1 Introduction

The phenomenon of sharp and weak emission lines (WELs) in optical spectra of middle to late B-type stars has been reported mainly in chemically peculiar (CP) stars. Detections of these weak features have been made possible by achieving both high spectral resolution and high signal-to-noise (SN) ratio observations. Sigut et al. (2000) reported detections of emission lines of Mn II, P II, and Hg II in the red spectral region of the helium-weak star 3 Cen A (B5 III-IVp). They also found very weak emission lines of Mn II in a mild HgMn star 46 Aql (B9 III). Sigut (2001a, b) carried out detailed analyses of emission lines of Mn II observed in 3 Cen A and 46 Aql and concluded that observations can be naturally explained by interlocked non-local thermodynamic equilibrium (NLTE) effect combined with the vertical stratification of the manganese abundance, with man-

ganese concentrated high in the photosphere.

Wahlgren and Hubrig (2000) reported detections of weak emission lines originating from high excitation states of Ti II, Cr II and Mn II in sharp lined late B-type stars including HgMn stars and suggested that these emission lines arise from a selective excitation process involving H Ly $\alpha$  photon energies. Sadakane et al. (2001) noted that all of the Ti II lines in 46 Aql with high excitation potential ( $\chi > 8.05$  eV) and large transition probabilities ( $\log gf > 0.1$ ) are observed in emission near 6000 Å. Wahlgren and Hubrig (2004) published an extensive list of emission lines of 3 Cen A. Their list includes emission line spectra of Si II, P II, Ca II, Mn II, Fe II, Ni II, Cu II, and Hg II. Abundances of 11 elements (from C to Hg) have been determined using a synthetic spectrum fitting technique.

Numerous weak emission lines of Cr II and Ti II have been

reported in a cool HgMn star HD 175640 (B9 V) by Castelli and Hubrig (2004). They noted that emission lines are selectively found for high excitation lines having large transition probabilities ( $\log gf > -1.0$ ) and that these emission lines are found in the red part ( $\lambda > 5850 \text{ \AA}$ ) of the spectrum. Castelli and Hubrig (2007) observed emission lines of Cr II, Mn II and Fe II and found isotopic anomalies for Ca and Hg in the Bp star HR 6000. They noted that there are disagreements between observed and calculated line strengths for some Fe II lines and suggest these discrepancies are due either to incorrect  $\log gf$  values or to the emission component filling the absorptions (filling-in effects).

Hubrig and González (2007) observed high resolution spectra of the sharp-lined magnetic helium-variable star a Cen (HD 125823) over the rotation period of 8.82 d and found variable high excitation S II, Mn II and Fe II emission lines. They found a correlation between the probable location of surface spots of Mn and Fe and the strength of the emission lines. It is interesting to notice that they note that an emission line detected in this star at  $6239.80 \text{ \AA}$  as an unidentified line (their table 1). Recently, Alexeeva et al. (2016) constructed a comprehensive model atom for C I and C II and computed the NLTE line formation for C I and C II. They analysed the lines of C I and C II in seven B to early A-type stars, including  $\iota$  Her, Sirius, and Vega, and found that the C I emission lines were detected in the four hottest stars, and these lines were well reproduced by their NLTE calculations.

Summarizing these published results, we notice that stars showing WELs are mainly middle B to early A-type stars including CP stars. Almost all WELs are arising from high excitation states of singly ionized ions. At the same time, WELs are found in the red and near-IR spectral regions preferentially and no WELs have been reported in the blue or in the near UV regions so far.

Nieva and Simón-Díaz (2011) analysed high resolution spectra of 13 early B-type main-sequence stars of spectral classes B0 V to B2 V and low projected rotational velocities ( $v \sin i < 60 \text{ km s}^{-1}$ ) in the Ori OB1 association. They published a graphical presentation of the spectrum of HD 35299 (B1.5 V) in the appendix. Nieva and Przybilla (2012) carried out a comprehensive spectral analyses of 27 B-type stars and published graphical presentations of spectra of four B-type stars including a B2 IV star  $\gamma$  Peg. Examining graphical data of HD 35299 (Nieva and Simón-Díaz 2011) and  $\gamma$  Peg (Nieva and Przybilla 2012), we noticed an emission like spike near  $6239.7 \text{ \AA}$  in both stars. Curiously, however, no identification has been given to this feature on graphs of both stars.

Interested in the nature of this unidentified feature, we examined high resolution spectral data of  $\gamma$  Peg obtained with the High-Dispersion Echelle Spectrograph (HIDES,  $R \sim 70000$ ) at the coudé focus of the 188-cm reflector of the Okayama Astrophysical Observatory (OAO) and data downloaded from

the Elodie archive ( $R \sim 42000$ , Moultaqa et al. 2004). We find that the emission like feature is definitely present on both data and conclude that the feature is not an observational artifact. We surveyed for candidate lines by simulating the spectrum and found two highly excited (12.84 eV) lines of Si II at  $6239.61$  and  $6239.66 \text{ \AA}$  are expected to appear as weak absorption lines in early B-type stars. Measured wavelength of the emission line just coincides with those of the two Si II lines. Furthermore, we found two additional weak emission features at  $6231.8 \text{ \AA}$  and at  $6243.4 \text{ \AA}$  in  $\gamma$  Peg. Observed wavelengths of these two features coincide with those of two highly excited (13.08 eV) lines of Al II at  $6231.75 \text{ \AA}$  and at  $6243.37 \text{ \AA}$ .

Because we can find no alternative identification for these features, we conclude that WELs of Al II and Si II are present in the optical region spectrum of  $\gamma$  Peg. This finding is the first case of WELs found not only in  $\gamma$  Peg but also in hot ( $T_{\text{eff}} > 20000 \text{ K}$ ) B-type stars.

We collected as many high resolution spectral data of early B-type stars as possible from various data archives, then tried a systematic survey for the Al II and Si II emission lines near  $6240 \text{ \AA}$  in these stars to find that the Si II emission line appears frequently in B2 - B3 sharp-lined main sequence stars while the Al II emission line appears in a narrower spectral range of B2-type stars. Details of our survey for WELs in early B-type stars and results are described in the following sections.

## 2 Observational data

We collected optical spectral data of 35 B-type stars of low rotational velocities corresponding to spectral types from B1 to B7 and luminosity classes from III to V from various data archives. Spectral data of 26 targets were observed using the HIDES spectrograph at OAO. Data of 11 targets were obtained with the Elodie spectrograph of the 193-cm telescope at the Observatoire de Haute Provence. Data were obtained by the UVES spectrograph of the ESO VLT (three targets) and by the High Dispersion Spectrograph (HDS) of the Subaru telescope (three targets). Raw data obtained by the HIDES and HDS spectrographs were downloaded from the SMOKA database, which is operated by the Astronomy Data Center, National Astronomical Observatory of Japan. Processed data of the Elodie and UVES spectrographs were obtained from the Elodie archive and the UVES-POP archive (Bagnulo et al. 2003), respectively.

The reduction of two-dimensional echelle spectral data obtained by the HIDES and HDS spectrographs (bias subtraction, flat-fielding, scattered-light subtraction, extraction of spectral data, and wavelength calibration) was performed in a standard manner using the IRAF software package. The wavelength calibration was done using the Th-Ar comparison spectra obtained during the observations. The observed wavelengths of all stars

observed by all four spectrographs have been converted into the laboratory scale using measured wavelengths of He I and Si II absorption lines. Finally, the continuum levels of all spectral data have been normalized to unity by a polynomial fitting technique.

Relevant data of our target objects are summarized in table 1. Spectral types are taken from the Bright Star Catalog 5-th edition (Hoffleit and Warren 1991), except for three stars (HD 89587, HD 133518 and HD 181858). Spectral types of two southern stars (HD 89587 and HD 133518) are taken from Houk (1978) and data of HD 181858 is taken from Houk and Swift (1999). Data of rotational velocities ( $v \sin i$ ) are taken from Abt et al. (2002). Data of  $v \sin i$  for five stars (HD 3360, HD 29248, HD 35039, HD35468, and HD36591) have been replaced with new data taken from Simón-Díaz and Herrero (2014) and that of HD 133518 is taken from Alecian et al. (2014). We could find no published data of  $v \sin i$  for HD 89587.

Effective temperatures ( $T_{\text{eff}}$ ) and surface gravities ( $\log g$ ) are taken from various sources. We adopt data given in Takeda et al. (2010) and Nieva (2013). When no data can be found in these two papers, we use  $T_{\text{eff}}$  and  $\log g$  values given in Lefever et al. (2010) (HD 35468 and HD 214993), Aerts et al. (2014) (HD 163472), Morel and Butler (2008) (HD 170580), and Alecian et al. (2014) (HD 133518). We can find neither published data of  $T_{\text{eff}}$  and  $\log g$  nor  $uvby$  and  $\beta$  photometric data for the southern star HD 89587. We estimated its effective temperature by comparing the line intensity ratio of the S II line at 5664.8 Å to the N II line at 5666.6 Å with those measured in 15 B2 and B3 type stars in table 1. The ratio is found to be sensitive to a change in temperature for stars belonging to spectral types B2 and B3. Measured equivalent widths (in mÅ) and central relative intensities (C. I.) of the Si II line at 6239.6 Å and the Al II line at 6243.4 Å are given in columns from 12 to 15. Measurements of equivalent widths are carried out using the direct integration method.

Figures 1 and 2 show spectral data near 6240 Å for five representative examples of hot B-type stars and five cooler stars, respectively. We plot observed and simulated spectra for each star. Simulated spectra were computed using the tabulated atmospheric parameters and the rotational velocity for each star, interpolating the ATLAS9 model atmospheres (Kurucz 1993). The solar abundances, the LTE line formation and the microturbulent velocity,  $\xi_t = 4 \text{ km s}^{-1}$ , have been assumed in these simulations. We use  $\log gf$  values of the Si II lines and the Al II lines taken from the NIST Atomic Database (Kramida et al. 2015), while  $\log gf$  values of other lines are taken from Kurucz and Bell (1995).

We surveyed for other emission features of high excitation Al II and Si II ions on a high SN ratio ( $\sim 900$ ) spectrum of  $\gamma$  Peg and found two and six additional emission features of these two ions, respectively, as listed in table 2. Figure 3 displays two

small sections of the spectra of two sharp lined stars  $\gamma$  Peg and  $\iota$  Her near the Si II line at 5688.81 Å (upper panel) and the Al II line at 5593.30 Å (lower panel). We can see that the Si II line is seen in emission in both stars. The Al II line appears as an emission feature in  $\gamma$  Peg, while the line is seen as a weak absorption feature in the cooler star  $\iota$  Her.

In figure 4, we compare observed profiles of the Si II emission line at 6239.6 Å and those of a low excitation (8.12 eV) absorption line of Si II at 6371.37 Å of three B2 type stars ( $\gamma$  Peg,  $\zeta$  Cas, and  $\gamma$  Ori) on the velocity scale.

### 3 Discussion

We have presented observations of weak emission lines (WELs) of high excitation Si II and Al II ions in the red region spectra of early B-type stars. WELs in hot B-type stars and those of Al II ions have not been reported in previous publications. We find that the emission line of Si II at 6239.6 Å is observed in all 13 stars in our sample contained in the  $T_{\text{eff}}$  range between 23000 K and 17500 K. The line is observed less frequently in middle B-type stars (between 17500 K and 16500 K) and the line is not observed in emission among cooler ( $T_{\text{eff}} < 16000$  K) stars. The observed high frequency of detection of the Si II line at 6239.6 Å in emission among early B-type stars strongly suggests that the occurrence of this emission line is not a rare case but a common phenomenon among these stars. The line of Al II at 6243.4 Å is observed in emission only in a narrow temperature range (between 23000 K and 19000 K) less frequently than the Si II line. The line is observed not in emission but as a weak absorption feature in stars with  $T_{\text{eff}} < 17500$  K. Data of equivalent widths of emission lines (table 1, columns 12 and 14) show that maxima of both emission lines are observed between the range in  $T_{\text{eff}}$  between 22000 K and 19500 K.

We have data of multi-epoch observations for two objects  $\gamma$  Peg and  $\iota$  Her, both of which show a clear emission line of Si II at 6239.6 Å. Data of six epochs (from 1998 November to 2006 October) and seven epochs (from 1994 April to 2013 June) are available for  $\gamma$  Peg and  $\iota$  Her, respectively. These data are obtained by the Elodie, HIDES, and HDS spectrographs. We examined averaged spectral data of each epoch of both stars and found no significant time variation in the line peak intensity, central wavelength, and width of the Si II emission line at 6239.6 Å. These data strongly suggest that the appearances of the emission line in these two stars are not temporal phenomena but they are stationary features lasting for at least a few decades.

Figure 4 clearly demonstrates that very faint WELs can be detected in a relatively fast rotating star such as  $\gamma$  Ori when using high SN and high resolution data. We can see from this figure that the emission lines show single-peaked and symmetric profiles in all three stars and that their line centers have no shift in wavelength with respect to those of low excitation ab-

sorption lines of Si II. Measured half widths of the emission lines are the same as those of low excitation absorption lines of Si II in all three stars. These observations imply that the faint WELs are formed nearly at the same location as the absorption lines and their origins are not circumstellar. Furthermore, the observed widths of WELs, which are the same as those of the rotationally broadened absorption lines, imply that the emitting gas is covering the whole stellar surface and is co-rotating with the star.

The mechanism for populating the highly excited states is still now under investigation. In a review article, Wahlgren (2008) noted that NLTE can be a significant mechanism for the production of WELs. Sigut and Lester (1996) carried out a theoretical work on near IR region WELs of Mg II in A and B-type stars and published predictions of line profiles of four Mg II lines between 1.01  $\mu\text{m}$  and 4.76  $\mu\text{m}$ . No observational confirmation of these Mg II emission lines has been published yet. Sigut (2001a, b) carried out analyses of emission lines of Mn II observed in 3 Cen A and 46 Aql and concluded that these emission lines can be explained by interlocked NLTE effect combined with the vertical stratification. Wahlgren and Hubrig (2000, 2004) proposed an alternative mechanism that the population of highly excited states might be due to excitation from the far-UV continuum radiation.

Our present sample covers a different temperature domain from that containing the previously known WELs stars on the HR diagram, and contains only one CP star (HD 133518: B2 IVp He-strong) and none of the remaining sample stars are known to show spectroscopic anomalies. Thus, it seems difficult to postulate a stratification of some specific elements, such as Si and Al, in their atmospheres. Thus, our results may have a significant bearing upon our understanding of the outermost atmospheric regions of B-type stars and the formation of the abundance anomalies observed in CP stars, which is generally attributed to the diffusion processes. Finally, we notice in table 1 that 12 stars belong to the  $\beta$  Cep type, the SPB type, or the hybrid type pulsational variable stars. The observed frequency of these variable stars among B-type stars is steadily increasing in recent years. Furthermore, weak magnetic fields have recently been detected in some of these variable stars (Wade et al. 2016).

We plan to carry out spectroscopic observations of early B-type stars in order to increase the number of sample stars. One of our interest is observing hot stars with spectral sub-types between B1 and B2, where we have only a few objects in the present sample. It might be possible to determine the hot end of the region in the  $T_{\text{eff}}$  range between 23000 K and 27000 K, in which the Si II line at 6239.6  $\text{\AA}$  appears as an emission line. We also plan to observe wavelength regions not included in the present study in order to survey for new emission features. These observations will provide useful boundary conditions or

constraints to be incorporated in theoretical interpretations.

This research has made use of the SIMBAD database, operated by CDS, Strasbourg, France. We thank Dr. E. Kambe for comments and Mr. Y. Notsu for his help in preparation of figure materials.

## References

- Abt, H. A., Levato, H., & Grosso, M. 2002, *ApJ*, 573, 359
- Aerts, C., Molenberghs, G., Kenward, M. G., & Neiner, C. 2014, *ApJ*, 781, 88
- Alecian, E., et al. 2014, *A&A*, 567, A28
- Alexeeva, S. A., Ryabchikova, T. A., & Mashonkina, L. I. 2016, *MNRAS*, 462, 1123
- Bagnulo, S., et al. 2003, *The Messenger* 114, 10
- Briquet, M., Neiner, C., Petit, P., Leroy, B., & de Batz, B. 2016, *A&A*, 587, A126
- Castelli, F., & Hubrig, S. 2004, *A&A*, 425, 263
- Castelli, F., & Hubrig, S. 2007, *A&A*, 475, 1041
- Hoffleit, D., & Warren, W. H. jr. 1991, *The Bright Star Catalog*, 5th Revised Edition, Astronomical Data Center, NSSDS/ADC
- Houk, N. 1978, *Michigan catalogue of two-dimensional spectral types for the HD stars*, Vol. 2, Dep. Astron., Univ. Michigan
- Houk, N., & Swift, C. 1999, *Michigan catalogue of two-dimensional spectral types for the HD Stars*, Vol. 5, Vol. 5, Dep. Astron., Univ. Michigan
- Hubrig, S., & González, J. F. 2007, *A&A*, 466, 1083
- Irrgang, A., Desphande, A., Moehler, S., Mugrauer, M., & Janousch, D. 2016, *A&A*, 591, L6
- Kramida, A., Ralchenko, Yu., Reader, J., & NIST ASD Team 2015, *NIST Atomic Spectra Database* (ver. 5.3), Available: <http://physics.nist.gov/asd>. National Institute of Standards and Technology, Gaithersburg, MD.
- Kurucz, R. L. 1993, *Kurucz CD-ROM*, No.13, ATLAS9 Stellar Atmosphere Programs and 2 km/s Grid, (Cambridge, MA: Harvard-Smithsonian Center for Astrophysics)
- Kurucz, R. L., & Bell, B. 1995, *Kurucz CD-ROM*, No.23, Atomic Line Data (Cambridge, MA: Harvard-Smithsonian Center for Astrophysics)
- Lefever, K., et al. 2010, *A&A*, 515, A74
- Moore, C. E. 1959, *Natl. Bur. Std. U.S. Tech. Note* (Office of Technical Services, U.S. Department of Commerce, Washington, D.C.), No. 36
- Moravveji, E. 2016, *MNRAS*, 455, L67
- Morel, T., & Butler, K. 2008, *A&A*, 487, 307
- Moultaka, J., Ilovaisky, S. A., Prugniel, P., & Soubiran, C. 2004, *PASP*, 116, 693
- Nieva, M. -F. 2013, *A&A*, 550, A26
- Nieva, M. -F., & Przybilla, N. 2012, *A&A*, 539, A143
- Nieva, M. -F., & Simón-Díaz, S. 2011, *A&A*, 532, A2
- Sadakane, K., et al. 2001, *PASJ*, 53, 1223
- Sigut, T. A. A. 2001a, *ApJ*, 546, L115
- Sigut, T. A. A. 2001b, *A&A*, 377, L27
- Sigut, T. A. A., Landstreet, J. D., & Shorlin, S. L. S. 2000, *ApJ*, 530, L89
- Sigut, T. A. A., & Lester, J. B. 1996, *ApJ*, 461, 972
- Simón-Díaz, S., & Herrero, A. 2014, *A&A*, 562, A135
- Stankov, A., & Handler, G. 2005, *ApJS*, 158, 193

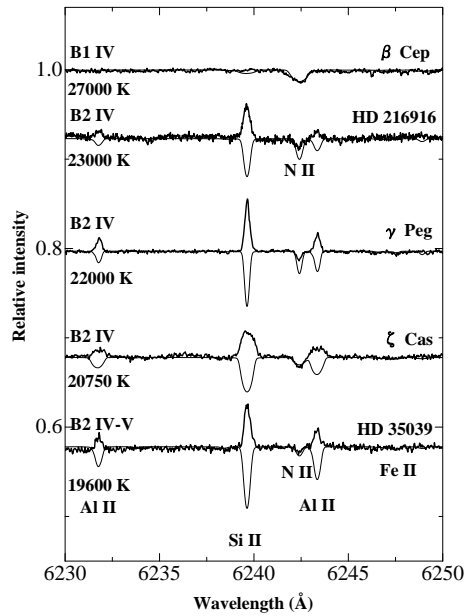


**Fig. 1.** Sample spectra of five hot (from B1 to B2) B-type stars between 6230 and 6250 Å. Lines of Si II at 6239.6 Å and of Al II at 6231.75 Å and at 6243.37 Å are shown. Spectral types and effective temperatures are indicated. Thick and thin lines show observed and simulated spectra, respectively.

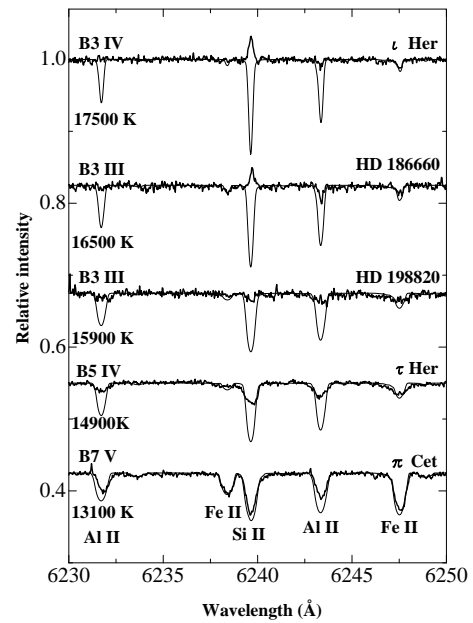


**Fig. 2.** The same as figure 1, but for five relatively cool (from B3 to B7) B-type stars.

Szewczuk, W., & Daszyńska-Daszkiewicz, J. 2015, MNRAS, 450, 1585  
 Takeda, Y., Kambe, E., Sadakane, K., & Masuda, S. 2010, PASJ, 62, 1239  
 Wade, G. A., et al. 2016, MNRAS, 456, 2  
 Wahlgren, G. M. 2008, Contrib. Astron. Obs. Skalnaté Pleso, 38, 279  
 Wahlgren, G. M., & Hubrig, S. 2000, A&A, 362, L13  
 Wahlgren, G. M., & Hubrig, S. 2004, A&A, 418, 1073

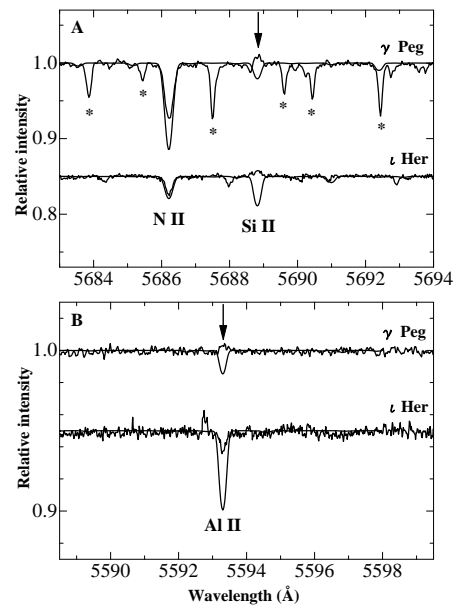


**Fig. 3.** Si II line at 5688.8 Å (panel A) and Al II line at 5593.3 Å (panel B) observed in  $\gamma$  Peg and  $\iota$  Her. Thick and thin lines show observed and simulated spectra, respectively. Asterisks indicate atmospheric absorption lines.



Table 1. Data of analysed stars

HD	Name	MK type	Variable type	$v \sin i$ $\text{km s}^{-1}$	Instrument	Obs. Date J. D. 2450000+	SN	$T_{\text{eff}}$ K	$\log g$ $\text{cm s}^{-2}$	Ref.	Si II 6239 E.W.	C.I.	Al II 6243 E.W.	C.I.
(1)	(2)	(3)	(4)	(5)	(6)	(7)	(8)	(9)	(10)	(11)	(12)	(13)	(14)	(15)
205021	$\beta$ Cep	B1 IV	$\beta$ Cep <sup>a</sup>	20	1,3	3257	800	27000	4.05	1	*	1.000	*	0.999
36591	HR 1861	B1 IV		9	3	3322	350	27000	4.12	1	*	1.005	*	0.997
216916	16 Lac	B2 IV	$\beta$ Cep <sup>a</sup>	10	2,3	2194	520	23000	3.95	1	-15	1.040	-3	1.008
214993	12 Lac	B2 III	Hybrid <sup>b</sup>	30	3	3015	440	23000	3.6	3	-11	1.012	*	0.999
163472	V2052 Oph	B2 IV-V	$\beta$ Cep <sup>a</sup>	75	3	2902	360	22490	3.95	4	-14	1.007	*	0.998
35468	$\gamma$ Ori	B2 III		52	3,4	2538	410	22000	3.6	3	-22	1.011	-4	1.002
29248	$\nu$ Eri	B2 III	Hybrid <sup>b</sup>	32	1	4030	380	22000	3.85	1	-12	1.006	*	1.001
886	$\gamma$ Peg	B2 IV	Hybrid <sup>b</sup>	0	1,3	4026	940	22000	3.95	1	-19	1.057	-6	1.020
16582	$\delta$ Cet	B2 IV	$\beta$ Cep <sup>a</sup>	5	3	1712	430	21250	3.8	1	-20	1.042	-6	1.013
3360	$\zeta$ Cas	B2 IV	SPB <sup>c</sup>	23	1,3	3301	650	20750	3.8	1	-21	1.027	-8	1.008
35708	$\sigma$ Tau	B2.5 IV		10	1	4030	460	20700	4.15	1	-15	1.020	-8	1.008
35039	$\sigma$ Ori	B2 IV-V		11	1	4030	520	19600	3.56	1	-20	1.048	-9	1.020
42690	HR 2205	B2 V		0	1	4030	410	19299	3.81	2	-17	1.030	-7	1.011
170580	HR 6941	B2V	Hybrid <sup>b</sup>	0	2	3184	970	19175	4.02	5	-13	1.039	*	1.001
133518	HIP 73966	B2 IVpHe		0	4	1983	270	19000	4.0	6	-10	1.053	-5	1.024
32249	$\psi$ Eri	B3 V		30	1	4027	510	18890	4.13	2	-4	1.005	*	1.000
34447	HR 1731	B3 IV		10	1	4027	270	18480	4.10	2	-8	1.021	*	1.000
160762	$\iota$ Her	B3 IV	SPB <sup>d</sup>	0	1,2,3	4026	610	17500	3.8	1	-9	1.030	+3	0.990
196035	HR 7862	B3 IV		20	1	4028	360	17499	4.36	2	+3	0.998	+3	0.996
43157	HR 2224	B5 V		30	1	4027	410	17486	4.12	2	+9	0.983	+5	0.993
223229	HR 9011	B3 IV		30	1	4026	370	17327	4.20	2	-8	1.005	*	0.999
89587	HIP 50519	B3 III		no data	4	2217	540	17000	no data	7	-6	1.016	+3	0.988
176502	V543 Lyr	B3 V		0	1	4027	390	16821	3.89	2	+6	0.986	+9	0.972
41753	$\nu$ Ori	B3 V		30	1	4029	410	16761	3.9	2	-4	1.005	*	0.994
25558	40 Tau	B3 V	SPB <sup>d</sup>	30	1	4028	390	16707	4.29	2	+9	0.982	+5	0.992
44700	HR 2292	B3 V		0	1	4029	340	16551	4.29	2	+6	0.982	+6	0.972
186660	HR 7516	B3 III		0	1	4027	310	16494	3.57	2	-6	1.025	+6	0.976
181858	HR 7347	B3 II-III		0	1	4027	270	16384	4.19	2	+9	0.979	+8	0.984
184171	8 Cyg	B3 IV		15	1	4027	430	15858	3.54	2	+6	0.988	+6	0.989
198820	HR 7996	B3 III		15	1	4027	280	15852	3.86	2	+6	0.989	+7	0.989
209008	18 Peg	B3 III	SPB <sup>e</sup>	5	1	4028	360	15800	3.75	1	+9	0.980	+12	0.982
28375	HR 1415	B3 V		0	1	4027	380	15278	4.30	2	+30	0.950	+20	0.971
11415	$\epsilon$ Cas	B3 III		30	1,3	4027	650	15174	3.54	2	+10	0.984	+14	0.986
147394	$\tau$ Her	B5 IV		30	1	4026	610	14898	4.01	2	+27	0.970	+18	0.980
17081	$\pi$ Cet	B7 V		25	1	4029	710	13063	3.72	2	+37	0.944	+20	0.966

(1) HD number, (2) Star name, (3) Spectral type, (4) References: a: Stankov and Handler (2005), b: Moravejji (2016), c: Briquet et al. (2016), d: Szewczuk and Daszyńska-Daszkiewicz (2015), and e: Irrgang et al. (2016). (5) Rotational velocity ( $v \sin i$ ). (6) Used spectrographs: 1: HIDES, 2: HDS, 3: Elodie, 4: UVES. (7) Date of observation in J. D. When multiple observations are available, date of observations used in measurements (12)–(15) are given. (8) SN ratio measured at the continuum level near 6250 Å. (9) Effective temperature. (10) Logarithm of surface gravity. (11) Sources of  $T_{\text{eff}}$  and  $\log g$ : 1: Nieva (2013), 2: Takeda et al. (2010), 3: Lefever et al. (2010), 4: Aerts et al. (2014), 5: Morel and Butler (2008), 6: Alecian et al. (2014), 7: Estimated using the S II and N II line intensity ratio. (12) and (14) Equivalent widths (E. W.) of the Si II 6239.6 and the Al II 6243.4 in mÅ. Data of emission and absorption features are given in negative and positive numbers, respectively. Entries marked with a colon(:) are less accurate. An asterisk (\*) indicates that no emission or absorption feature can be recognized. (13) and (15) Central intensities (C. I.) of the Si II 6239.6 and the Al II 6243.4 lines relative to the local continuum level.

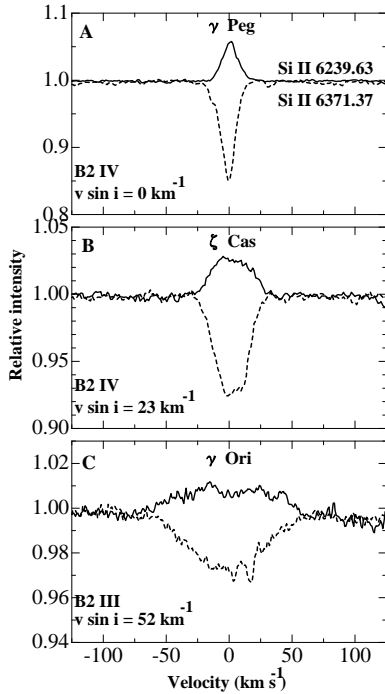


Fig. 4. Profiles of the Si II emission line at 6239.6 Å (thick lines) and those of low excitation Si II absorption line at 6371.37 Å (broken lines) for three B2 type stars  $\gamma$  Peg (panel A),  $\zeta$  Cas (panel B), and  $\gamma$  Ori (panel C). Spectral types and data of  $v \sin i$  are indicated. Profiles are plotted on the velocity scale.

Table 2. Emission lines of Al II and Si II observed in  $\gamma$  Peg

Ion	Mult. No.	$\lambda$ (Å)	Excitation potential (eV)	Configuration Upper	Lower	$\log gf$	Peak intensity
Al II	–	5593.30	13.26	$3s4p$	$3s4d$	0.337	1.003
	10	6226.18	13.07	$3s4p$	$3s4d$	0.037	1.004
	10	6231.75	13.07	$3s4p$	$3s4d$	0.389	1.014
	10	6243.36	13.08	$3s4p$	$3s4d$	0.659	1.020
Si II	–	5185.52	12.84	$3s^24f$	$3s^27g$	-0.302	1.013
	–	5185.56	12.84	$3s^24f$	$3s^27g$	-0.456	1.013
	–	5466.43	12.53	$3s^24d$	$3s^26f$	-0.237	1.016
	–	5466.89	12.53	$3s^24d$	$3s^26f$	-0.082	1.012
	–	5688.81	14.19	$3s3p(^3P^o)3d$	$3s3p(^3P^o)4p$	0.126	1.009
	–	5701.37	14.17	$3s3p(^3P^o)3d$	$3s3p(^3P^o)4p$	-0.057	1.004
	–	6239.61	12.84	$3s^24f$	$3s^26g$	0.177	1.057
–	6239.66	12.84	$3s^24f$	$3s^26g$	0.021	1.057	

Multiplet numbers are taken from Moore (1959) and atomic data (wavelengths  $\lambda$ , excitation potentials, electron configurations and  $\log gf$  values) are taken from the NIST atomic database.